Kittel
Chapter 9

Part 4

EXPERIMENTAL METHODS IN FERMI SURFACE STUDIES

Powerful experimental methods have been developed for the determination of Fermi surfaces. The methods include magnetoresistance, anomalous skin effect, cyclotron resonance, magneto-acoustic geometric effects, the Shubnikow-de Haas effect, and the de Haas-van Alphen effect. Further information on the momentum distribution is given by positron annihilation, Compton scattering, and the Kohn effect.

We propose to study one method rather thoroughly. All the methods are useful, but all need detailed theoretical analysis and are not for beginners. We select the de Haas-van Alphen effect because it exhibits very well the characteristic periodicity in $1/B$ of the properties of a metal in a uniform magnetic field.

Quantization of Orbits in a Magnetic Field

The momentum $\mathbf{p}$ of a particle in a magnetic field is the sum (Appendix G) of two parts, the kinetic momentum $\mathbf{p}_{\text{kin}} = m\mathbf{v} = \hbar\mathbf{k}$ and the potential momentum or field momentum $\mathbf{p}_{\text{field}} = q\mathbf{A}/c$, where q is the charge. The vector potential is related to the magnetic field by $\mathbf{B} = \text{curl } \mathbf{A}$. The total momentum is

(CGS)
$$\mathbf{p} = \mathbf{p}_{\text{kin}} + \mathbf{p}_{\text{field}} = \hbar\mathbf{k} + q\mathbf{A}/c \ . \tag{22}$$

In SI the factor c^{-1} is omitted.

Following the semiclassical approach of Onsager and Lifshitz, we assume that the orbits in a magnetic field are quantized by the Bohr-Sommerfeld relation

$$\oint \mathbf{p} \cdot d\mathbf{r} = (n + \gamma)2\pi\hbar \ , \tag{23}$$

when n is an integer and γ is a phase correction that for free electrons has the value $\frac{1}{2}$. Then

$$\oint \mathbf{p} \cdot d\mathbf{r} = \oint \hbar\mathbf{k} \cdot d\mathbf{r} + \frac{q}{c}\oint \mathbf{A} \cdot d\mathbf{r} \ . \tag{24}$$

The equation of motion of a particle of charge q in a magnetic field is

$$\hbar \frac{d\mathbf{k}}{dt} = \frac{q}{c} \frac{d\mathbf{r}}{dt} \times \mathbf{B} \ . \tag{25a}$$

We integrate with respect to time to give

$$\hbar \mathbf{k} = \frac{q}{c} \mathbf{r} \times \mathbf{B} \ ,$$

apart from an additive constant which does not contribute to the final result.

Thus one of the path integrals in (24) is

$$\oint \hbar \mathbf{k} \cdot d\mathbf{r} = \frac{q}{c} \oint \mathbf{r} \times \mathbf{B} \cdot d\mathbf{r} = -\frac{q}{c} \mathbf{B} \cdot \oint \mathbf{r} \times d\mathbf{r} = -\frac{2q}{c} \Phi \ , \tag{25b}$$

where Φ is the magnetic flux contained within the orbit in real space. We have used the geometrical result that

$$\oint \mathbf{r} \times d\mathbf{r} = 2 \times (\text{area enclosed by the orbit}) \ .$$

The other path integral in (24) is

$$\frac{q}{c}\oint \mathbf{A}\cdot d\mathbf{r} = \frac{q}{c}\int \mathbf{curl}\ \mathbf{A}\cdot d\boldsymbol{\sigma} = \frac{q}{c}\int \mathbf{B}\cdot d\boldsymbol{\sigma} = \frac{q}{c}\Phi\ , \tag{25c}$$

by the Stokes theorem; here $d\boldsymbol{\sigma}$ is the area element in real space. The momentum path integral is the sum of (25b) and (25c):

$$\oint \mathbf{p}\cdot d\mathbf{r} = -\frac{q}{c}\Phi = (n+\gamma)2\pi\hbar\ . \tag{26}$$

It follows that the orbit of an electron is quantized in such a way that the flux through it is

For orbit in real space

$$\Phi_n = (n+\gamma)(2\pi\hbar c/e)\ . \tag{27}$$

The flux unit $2\pi\hbar c/e = 4.14\times 10^{-7}$ gauss cm^2 or T m^2.

In the de Haas-van Alphen effect discussed below we need the area of the orbit in wavevector space. We obtained in (27) the flux through the orbit in real space. By (25a) we know that a line element Δr in the plane normal to $\mathbf{B}$ is related to Δk by $\Delta r = (\hbar c/eB)\,\Delta k$, so that the area S_n in $\mathbf{k}$ space is related to the area A_n of the orbit in $\mathbf{r}$ space by

$$A_n = (\hbar c/eB)^2 S_n \ . \tag{28}$$

It follows that $\Phi_n = A_n B$

$$\Phi_n = \left(\frac{\hbar c}{e}\right)^2 \frac{1}{B} S_n = (n + \gamma)\frac{2\pi\hbar c}{e} \tag{29}$$

From Eq. (27)

from (27), whence the area of an orbit in $\mathbf{k}$ space will satisfy

$$S_n = (n + \gamma)\frac{2\pi e}{\hbar c} B \ . \tag{30}$$

In Fermi surface experiments we may be interested in the increment ΔB for which two successive orbits, n and $n + 1$, have the same area in $\mathbf{k}$ space on the Fermi surface. The areas are equal when

From eq. 30

$$S\left(\frac{1}{B_{n+1}} - \frac{1}{B_n}\right) = \frac{2\pi e}{\hbar c}\ , \tag{31}$$

from (30). We have the important result that equal increments of $1/B$ reproduce similar orbits—this periodicity in $1/B$ is a striking feature of the magneto-oscillatory effects in metals at low temperatures: resistivity, susceptibility, heat capacity.

The population of orbits on or near the Fermi surface oscillates as B is varied, causing a wide variety of effects. From the period of the oscillation we reconstruct the Fermi surface. The result (30) is independent of the gauge of the vector potential used in the expression (22) for momentum; that is, $\mathbf{p}$ is not gauge invariant, but S_n is. Gauge invariance is discussed further in Chapter 12 and in Appendix G.

De Haas-van Alphen Effect

The de Haas-van Alphen effect is the oscillation of the magnetic moment of a metal as a function of the static magnetic field intensity. The effect can be observed in pure specimens at low temperatures in strong magnetic fields: we do not want the quantization of the electron orbits to be blurred by collisions, and we do not want the population oscillations to be averaged out by thermal population of adjacent orbits.

The analysis of the dHvA effect is given for absolute zero in Fig. 23. The electron spin is neglected. The treatment is given for a two-dimensional (2D) system; in 3D we need only multiply the 2D wavefunction by plane wave factors $\exp(ik_z z)$, where the magnetic field is parallel to the z axis. The area of an orbit in k_x, k_y space is quantized as in (30). The area between successive orbits is

From eq. (30)

$$\Delta S = S_n - S_{n-1} = 2\pi eB/\hbar c \ . \qquad (32)$$

Also see Fig. 24

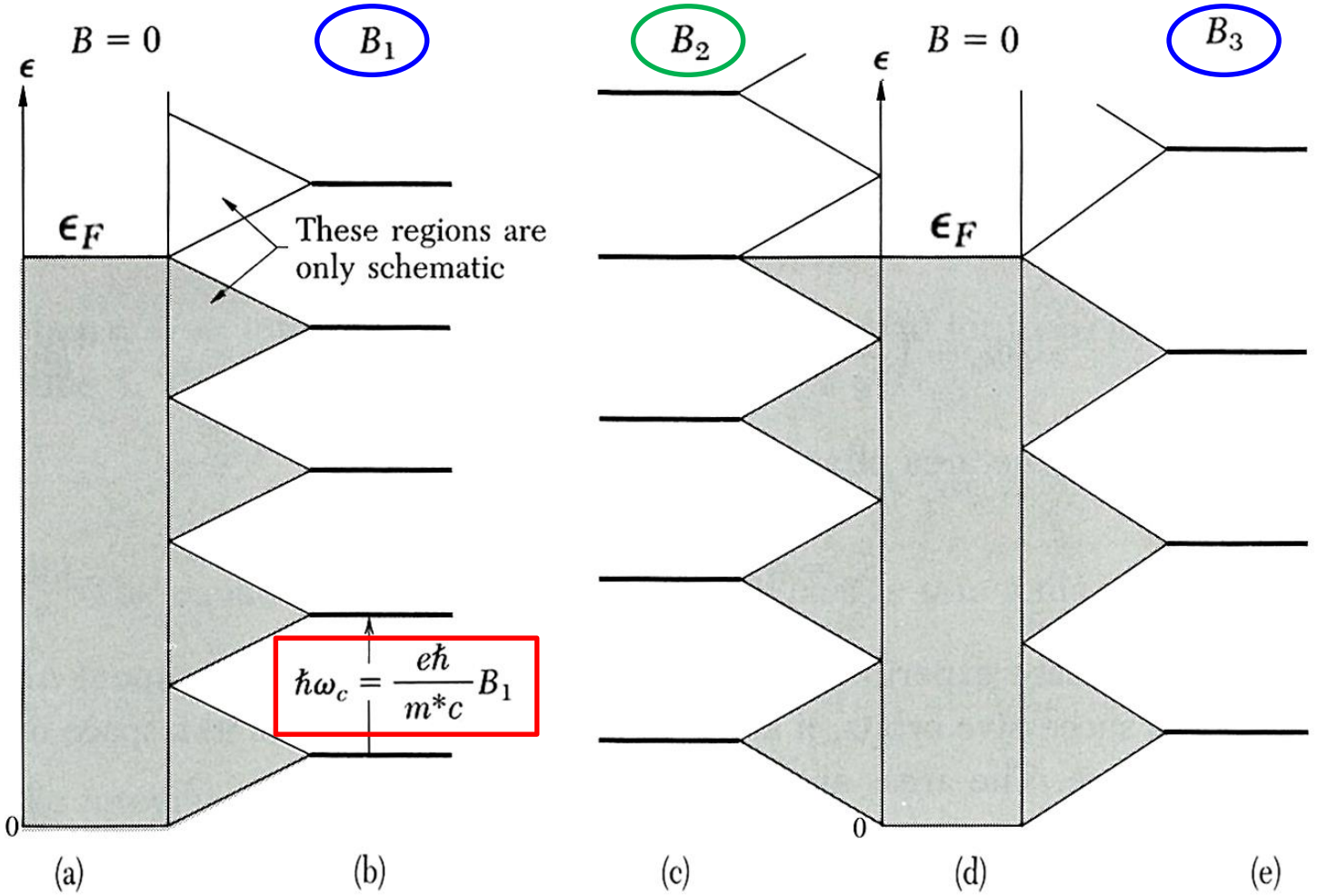

Figure 23 Explanation of the de Haas-van Alphen effect for a free electron gas in two dimensions in a magnetic field. The filled orbitals of the Fermi sea in the absence of a magnetic field are shaded in *a* and *d*. The energy levels in a magnetic field are shown in *b*, *c*, and *e*. In *b* the field has a value B_1 such that the total energy of the electrons is the same as in the absence of a magnetic field: as many electrons have their energy raised as lowered by the orbital quantization in the magnetic field B_1. When we increase the field to B_2 the total electron energy is increased, because the uppermost electrons have their energy raised. In *e* for field B_3 the energy is again equal to that for the field $B = 0$. The total energy is a minimum at points such as B_1, B_3, B_5, . . . , and a maximum near points such as B_2, B_4, ...

The area in **k** space occupied by a single orbital is $(2\pi/L)^2$, neglecting spin, for a square specimen of side L. Using (32) we find that the number of free electron orbitals that coalesce in a single magnetic level is

Degeneracy

$$D = (2\pi eB/\hbar c)(L/2\pi)^2 = \rho B \ , \tag{33}$$

where $\rho = eL^2/2\pi\hbar c$, as in Fig. 24. Such a magnetic level is called a **Landau level**.

The dependence of the Fermi level on B is dramatic. For a system of N electrons at absolute zero the Landau levels are entirely filled up to a magnetic quantum number we identify by s, where s is a positive integer. Orbitals at the next higher level $s + 1$ will be partly filled to the extent needed to accommodate the electrons. The Fermi level will lie in the Landau level $s + 1$ if there are electrons in this level; as the magnetic field is increased the electrons move to lower levels. When $s + 1$ is vacated, the Fermi level moves down abruptly to the next lower level s.

In a magnetic field

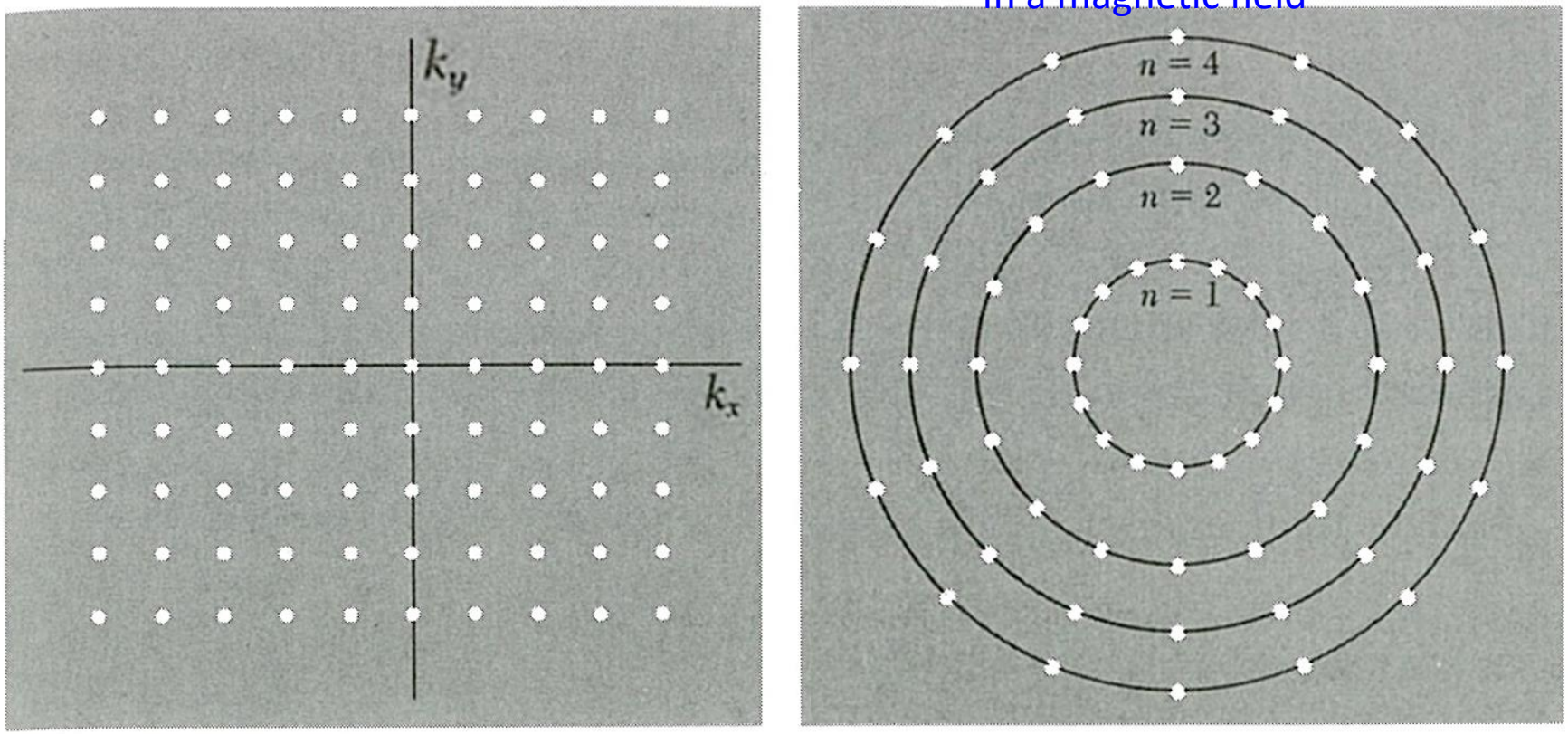

Figure 24 (a) Allowed electron orbitals in two dimensions in absence of a magnetic field. (b) In a magnetic field the points which represent the orbitals of free electrons may be viewed as restricted to circles in the former $k_x k_y$ plane. The successive circles correspond to successive values of the quantum number n in the energy $(n - \frac{1}{2})k\omega_c$. The area between successive circles is

illustration of Eq. 24 $\pi\Delta(k^2) = 2\pi k(\Delta k) = (2\pi m/\hbar^2)\,\Delta\epsilon = 2\pi m\omega_c/\hbar = 2\pi eB/\hbar c$ $\Delta\varepsilon = \hbar\omega_c$ $\omega_c = eB/m^*c$

The angular position of the points has no significance. The number of orbitals on a circle is constant and is equal to the area between successive circles times the number of orbitals per unit area in (a), or $(2\pi eB/\hbar c)(L/2\pi)^2 = L^2 eB/2\pi\hbar c$, neglecting electron spin.

The electron transfer to lower Landau levels can occur because their degeneracy D increases as B is increased, as shown in Fig. 25. As B is increased there occur values of B at which the quantum number of the uppermost filled level decreases abruptly by unity. At the critical magnetic fields labeled B_s no level is partly occupied at absolute zero, so that

$$s\rho B_s = N \ . \tag{34}$$

The number of filled levels times the degeneracy at B_s must equal the number of electrons N.

To show the periodicity of the energy as B is varied, we use the result that the energy of the Landau level of magnetic quantum number n is $E_n = (n - \frac{1}{2})\hbar\omega_c$, where $\omega_c = eB/m^*c$ is the cyclotron frequency. The result for E_n follows from the analogy between the cyclotron resonance orbits and the simple harmonic oscillator, but now we have found it convenient to start counting at $n = 1$ instead of at $n = 0$.

$s\rho\, B_s = N$

$(1/B_s)N = s\rho$

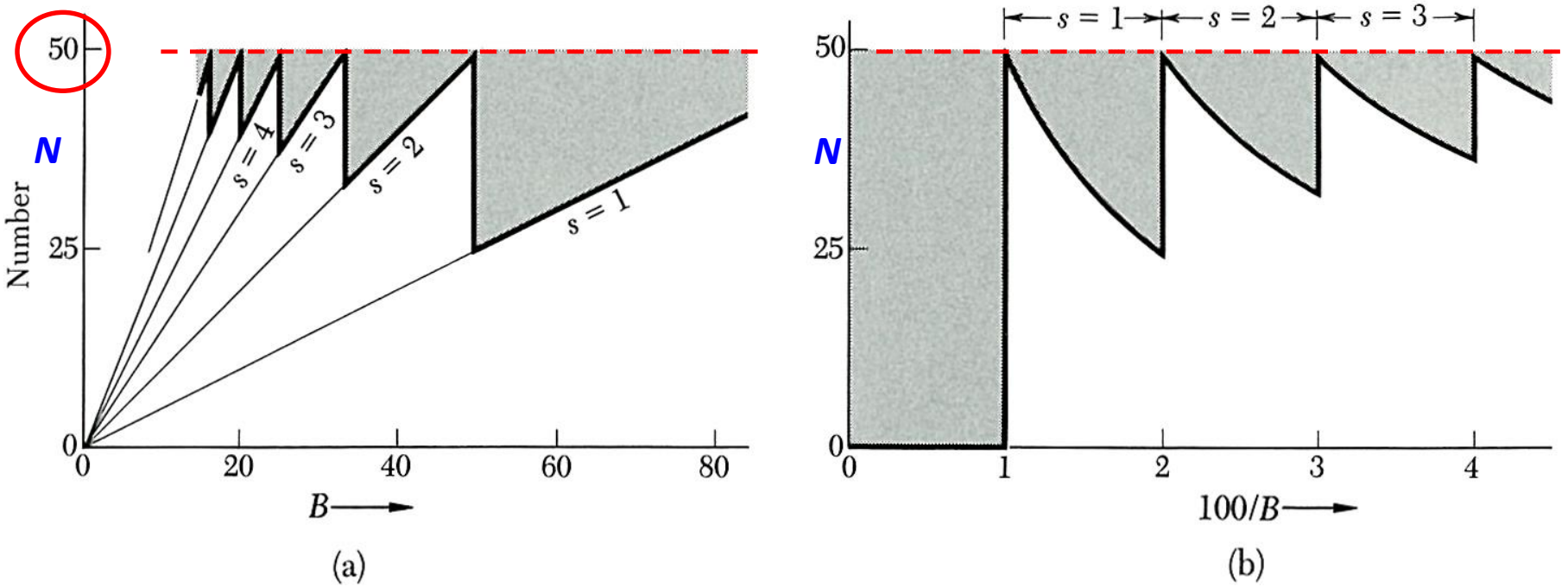

Figure 25 (a) The heavy line gives the number of particles in levels which are completely occupied in a magnetic field B, for a two-dimensional system with $N = 50$ and $\rho = 0.50$. The shaded area gives the number of particles in levels partially occupied. The value of s denotes the quantum number of the highest level which is completely filled. Thus at $B = 40$ we have $s = 2$: the levels $n = 1$ and $n = 2$ are filled and there are 10 particles in the level $n = 3$. At $B = 50$ the level $n = 3$ is empty. (b) The periodicity in $1/B$ is evident when the same points are plotted against $1/B$.

s = 2, D = 40;

s = 3, N_3= 50 - 40 = 10

The total energy of the electrons in levels that are fully occupied is

$$\sum_{n=1}^{s} D\hbar\omega_c(n - \tfrac{1}{2}) = \tfrac{1}{2}D\hbar\omega_c s^2 \ , \qquad (35)$$

D = ρ B

where D is the number of electrons in each level. The total energy of the electrons in the partly occupied level $s + 1$ is

$$\hbar\omega_c(s + \tfrac{1}{2})(N - sD) \ , \qquad (36)$$

Function of B^2 & B

where sD is the number of electrons in the lower filled levels. The total energy of the N electrons is the sum of (35) and (36), as in Fig. 26.

The magnetic moment μ of a system at absolute zero is given by $\mu = -\partial U/\partial B$. The moment here is an oscillatory function of $1/B$, Fig. 27. This oscillatory magnetic moment of the Fermi gas at low temperatures is the de Haas-van Alphen effect. From (31) we see that the oscillations occur at equal intervals of $1/B$ such that

$$\Delta\left(\frac{1}{B}\right) = \frac{2\pi e}{\hbar c S} \ , \qquad (37)$$

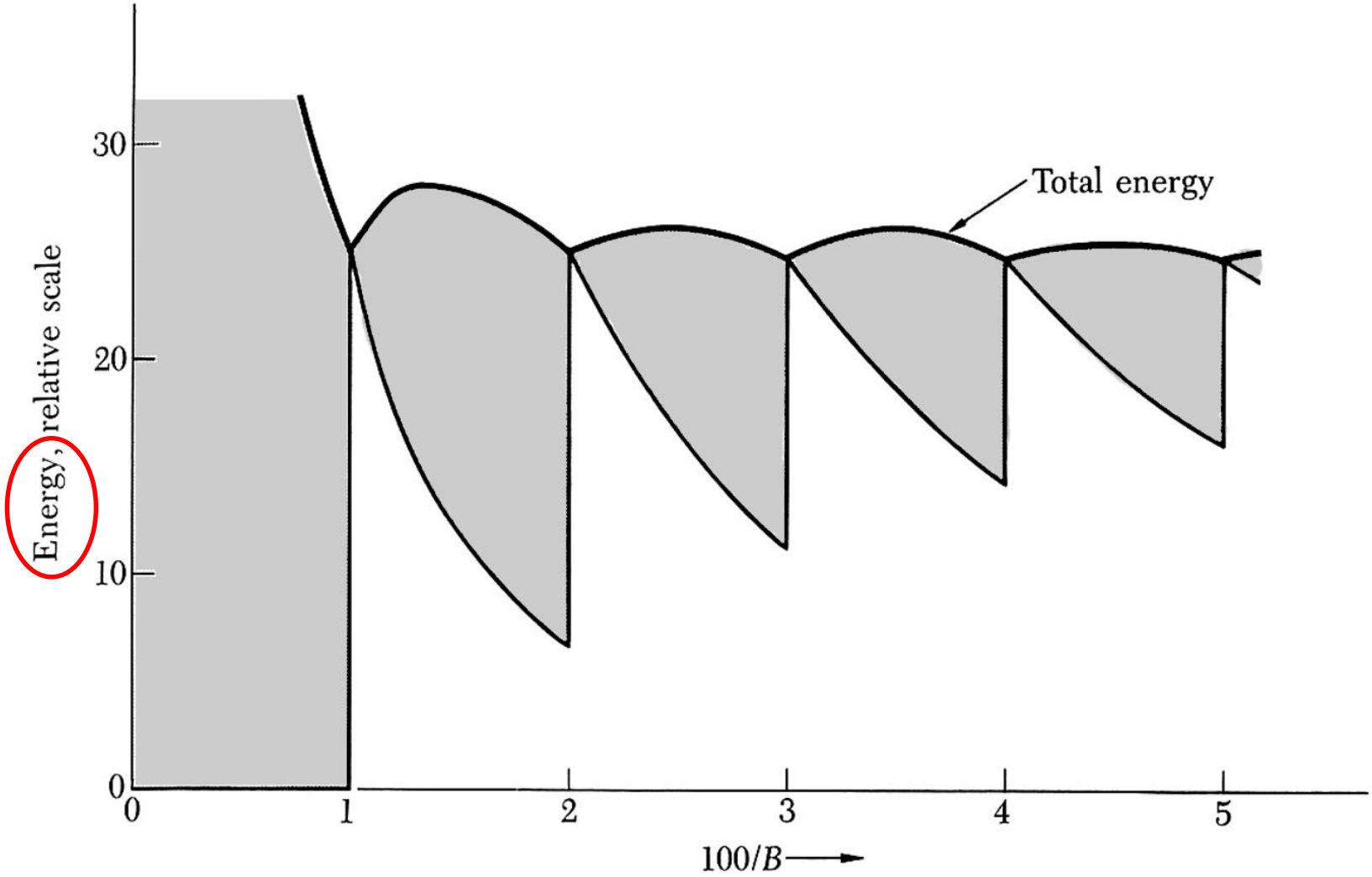

Figure 26 The upper curve is the total electronic energy versus $1/B$. The oscillations in the energy U may be detected by measurement of the magnetic moment, given by $-\partial U/\partial B$. The thermal and transport properties of the metal also oscillate as successive orbital levels cut through the Fermi level when the field is increased. The shaded region in the figure gives the contribution to the energy from levels that are only partly filled. The parameters for the figure are the same as for Fig. 25, and we have taken the units of B such that $B = \hbar\omega_c$.

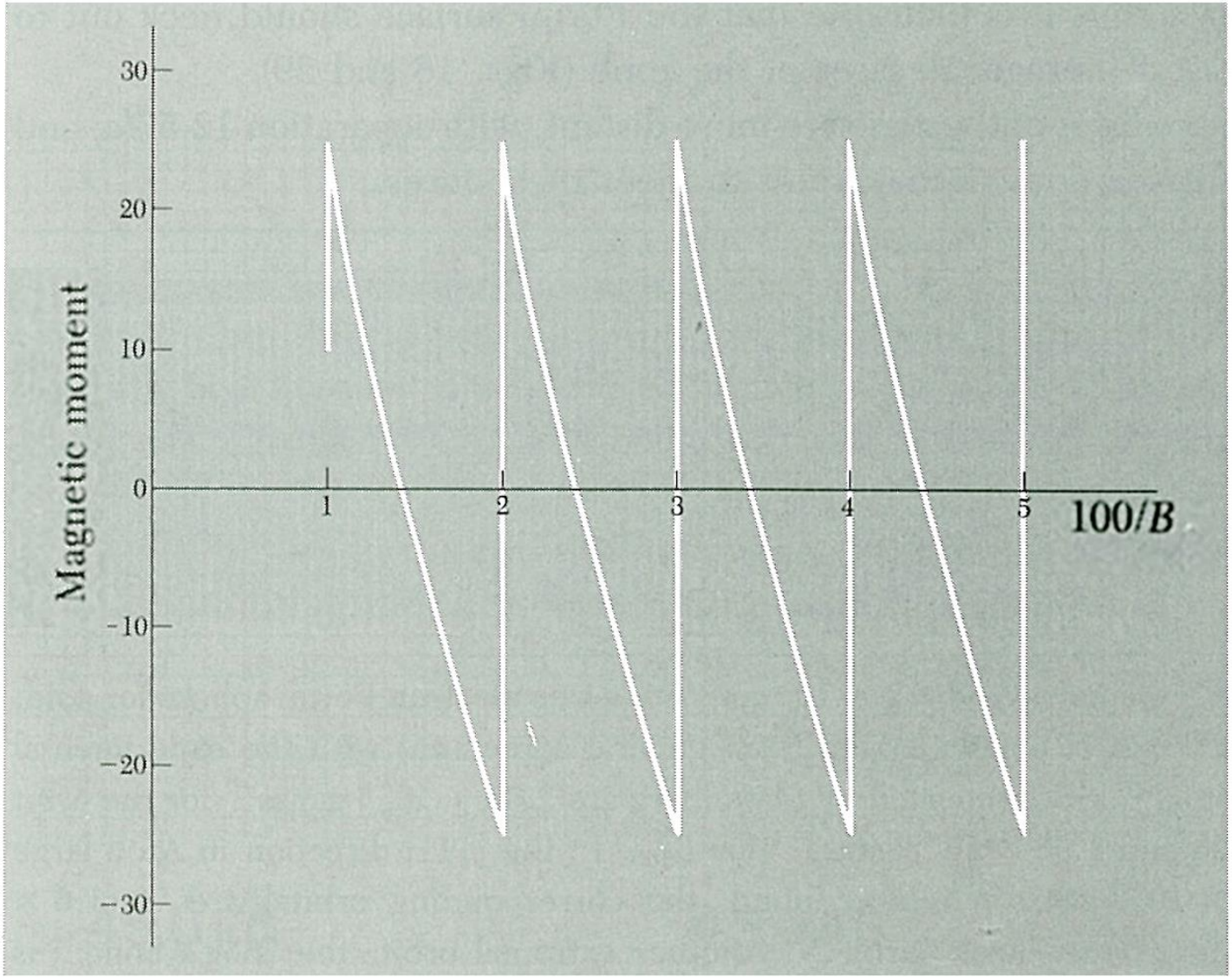

Figure 27 At absolute zero the magnetic moment is given by $-\partial U/\partial B$. The energy plotted in Fig. 26 leads to the magnetic moment shown here, an oscillatory function of $1/B$. In impure specimens the oscillations are smudged out in part because the energy levels are no longer sharply defined.

where S is the extremal area (see below) of the Fermi surface normal to the direction of **B**. From measurements of $\Delta(1/B)$, we deduce the corresponding extremal areas S; thereby much can be inferred about the shape and size of the Fermi surface.

Extremal Orbits. One point in the interpretation of the dHvA effect is subtle. For a Fermi surface of general shape the sections at different values of k_B will have different periods. The response will be the sum of contributions from all sections or all orbits. *But the dominant response of the system comes from orbits whose periods are stationary with respect to small changes in* k_B. Such orbits are called **extremal orbits**. Thus in Fig. 28 the section AA' dominates the observed cyclotron period.

The argument can be put in mathematical form, but we do not give the proof here (*QTS*, p. 223; Ziman, p. 322). Essentially it is a question of phase cancellation: the contributions of different nonextremal orbits cancel, but near the extrema the phase varies only slowly and there is a net signal from these orbits. Sharp resonances are obtained even from complicated Fermi surfaces because the experiment selects the extremal orbits.

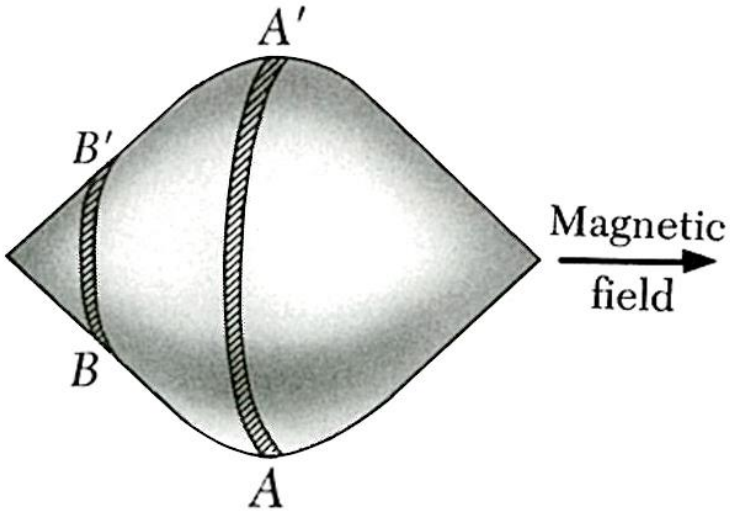

Figure 28 The orbits in the section AA' are extremal orbits: the cyclotron period is roughly constant over a reasonable section of the Fermi surface. Other sections such as BB' have orbits that vary in period along the section.

Fermi Surface of Copper. The Fermi surface of copper is distinctly nonspherical: eight necks make contact with the hexagonal faces of the first Brillouin zone of the fcc lattice. The electron concentration in a monovalent metal with an fcc structure is $n = 4/a^3$: there are four electrons in a cube of volume a^3. The radius of a free electron Fermi sphere is

$$k_F = (3\pi^2 n)^{1/3} = (12\pi^2/a^3)^{1/3} \cong (4.90/a) \ , \tag{38}$$

and the diameter is $9.80/a$.

The shortest distance across the Brillouin zone (the distance between hexagonal faces) is $(2\pi/a)(3)^{1/2} = 10.88/a$, somewhat larger than the diameter of the free electron sphere. The sphere does not touch the zone boundary, but we know that the presence of a zone boundary tends to lower the band energy near the boundary. Thus it is plausible that the Fermi surface should neck out to meet the closest (hexagonal) faces of the zone (Figs. 18 and 29).

The square faces of the zone are more distant, with separation $12.57/a$, and the Fermi surface does not neck out to meet these faces.

Cu

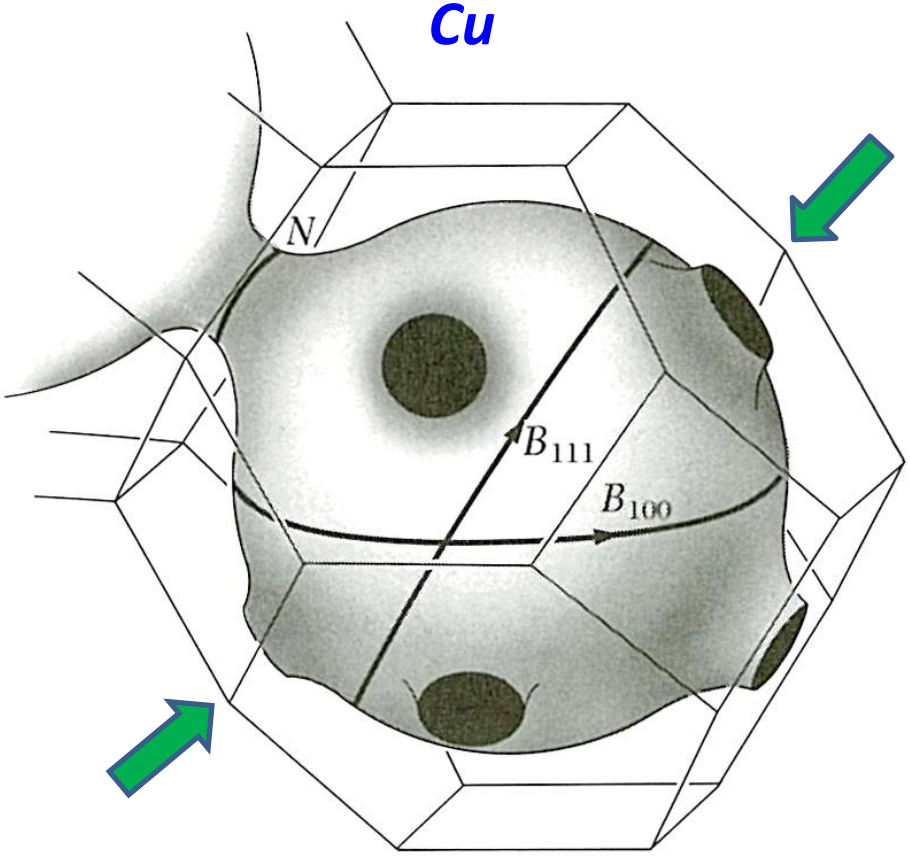

Figure 29 Fermi surface of copper, after Pippard. The Brillouin zone of the fcc structure is the truncated octahedron derived in Chapter 2. The Fermi surface makes contact with the boundary at the center of the hexagonal faces of the zone, in the [111] directions in **k** space. Two "belly" extremal orbits are shown, denoted by *B*; the extremal "neck" orbit is denoted by *N*.

Cu or Au

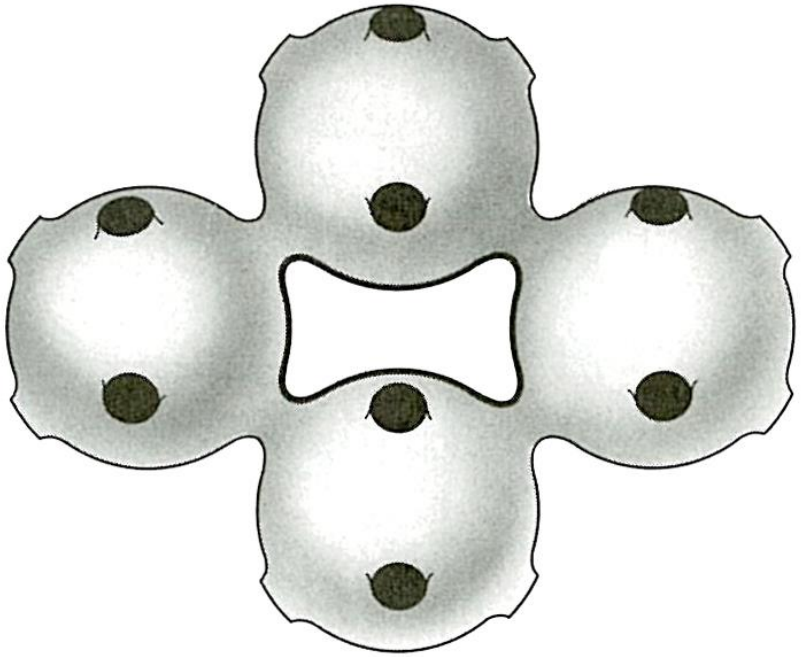

Figure 30 Dog's bone orbit of an electron on the Fermi surface of copper or gold in a magnetic field. This orbit is classified as holelike because the energy increases toward the interior of the orbit.

Au

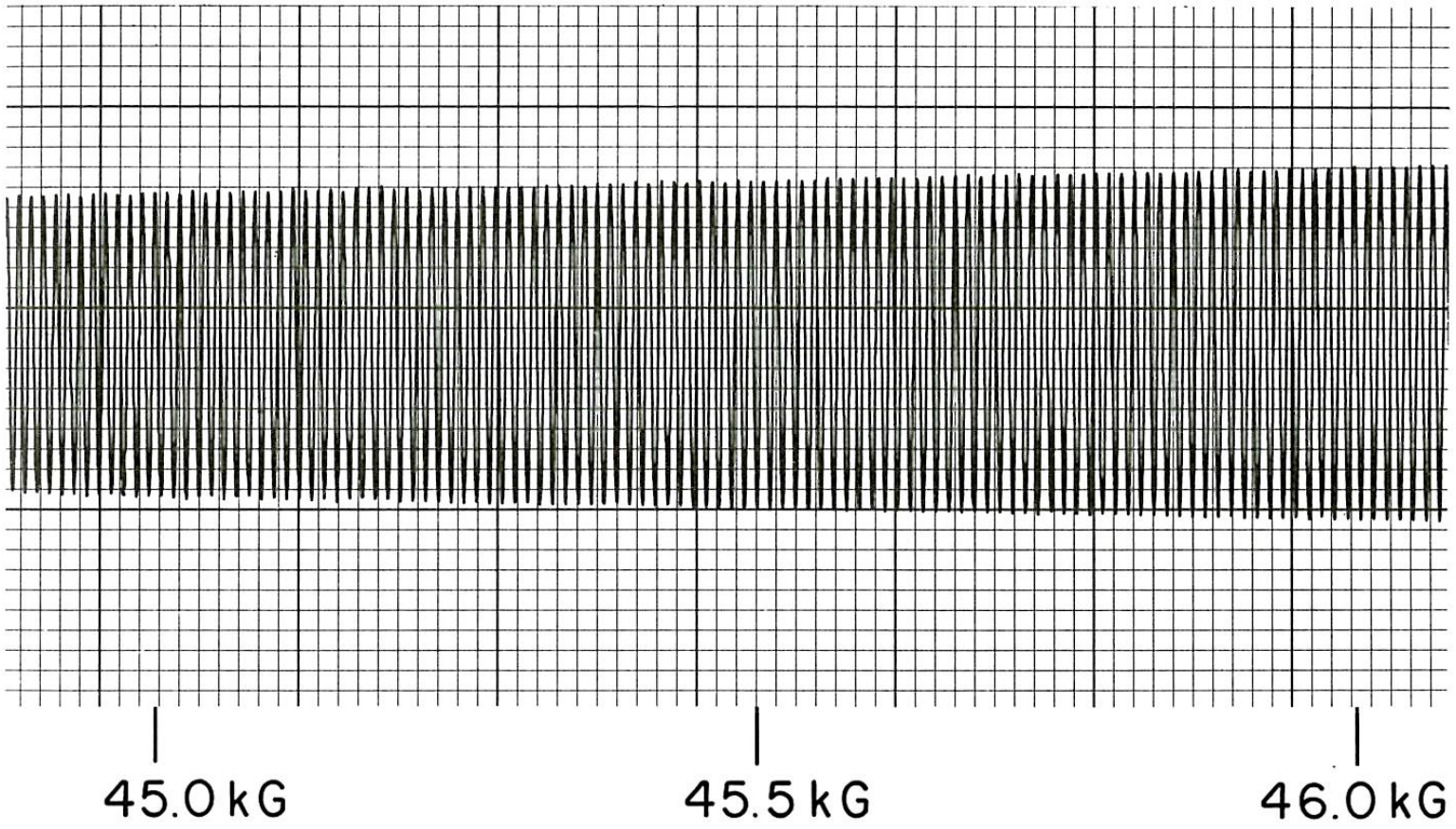

Figure 31 De Haas-van Alphen effect in gold with **B** ∥ [110]. The oscillation is from the dog's bone orbit of Fig. 30. The signal is related to the second derivative of the magnetic moment with respect to field. The results were obtained by a field modulation technique in a high-homogeneity superconducting solenoid at about 1.2 K. (Courtesy of I. M. Templeton.)

Au

EXAMPLE: ***Fermi Surface of Gold.*** In gold for quite a wide range of field directions Shoenberg finds the magnetic moment has a period of 2×10^{-9} gauss^{-1}. This period corresponds to an extremal orbit of area

$$S = \frac{2\pi e/\hbar c}{\Delta(1/B)} \cong \frac{9.55 \times 10^{7}}{2 \times 10^{-9}} \cong 4.8 \times 10^{16} \text{ cm}^{-2} \ .$$

From Table 6.1, we have $k_F = 1.2 \times 10^{8}$ cm^{-1} for a free electron Fermi sphere for gold, or an extremal area of 4.5×10^{16} cm^{-2}, in general agreement with the experimental value. The actual periods reported by Shoenberg are 2.05×10^{-9} gauss^{-1} for the orbit B_{111} of Fig. 28 and 1.95×10^{-9} gauss^{-1} for B_{100}. In the [111] direction in Au a large period of 6×10^{-8} gauss^{-1} is also found; the corresponding orbital area is 1.6×10^{15} cm^{-2}. This is the "neck" orbit *N*. Another extremal orbit, the "dog's bone," is shown in Fig. 30; its area in Au is about 0.4 of the belly area. Experimental results are shown in Fig. 31. To do the example in SI, drop c from the relation for S and use as the period 2×10^{-5} tesla^{-1}.

The free electron Fermi sphere of aluminum fills the first zone entirely and has a large overlap into the second and third zones, Fig. 1. The third zone Fermi surface is quite complicated, even though it is just made up of certain pieces of the surface of the free electron sphere. The free electron model also gives small pockets of holes in the fourth zone, but when the lattice potential is taken into account these empty out, the electrons being added to the third zone. The general features of the predicted Fermi surface of aluminum are quite well verified by experiment. Figure 32 shows part of the free electron Fermi surface of magnesium.

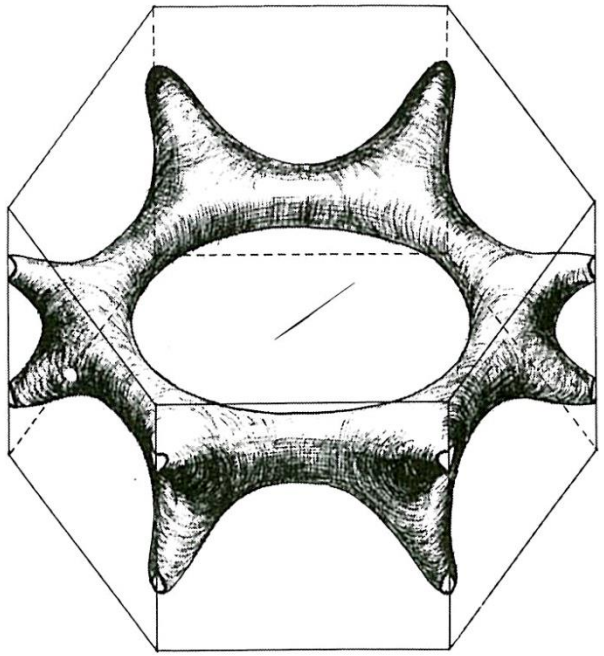

hcp ***Mg***

Figure 32 Multiply-connected hole surface of magnesium in bands 1 and 2, according to L. M. Falicov. (Drawing by Marta Puebla.)

Magnetic Breakdown. Electrons in sufficiently high magnetic fields will move in free particle orbits, the circular cyclotron orbits of Fig. 33a. Here the magnetic forces are dominant, and the lattice potential is a slight perturbation. In this limit the classification of the orbitals into bands may have little importance. However, we know that at low magnetic fields the motion is described by (8.7) with the band structure $\epsilon_{\mathbf{k}}$ that obtains in the absence of a magnetic field.

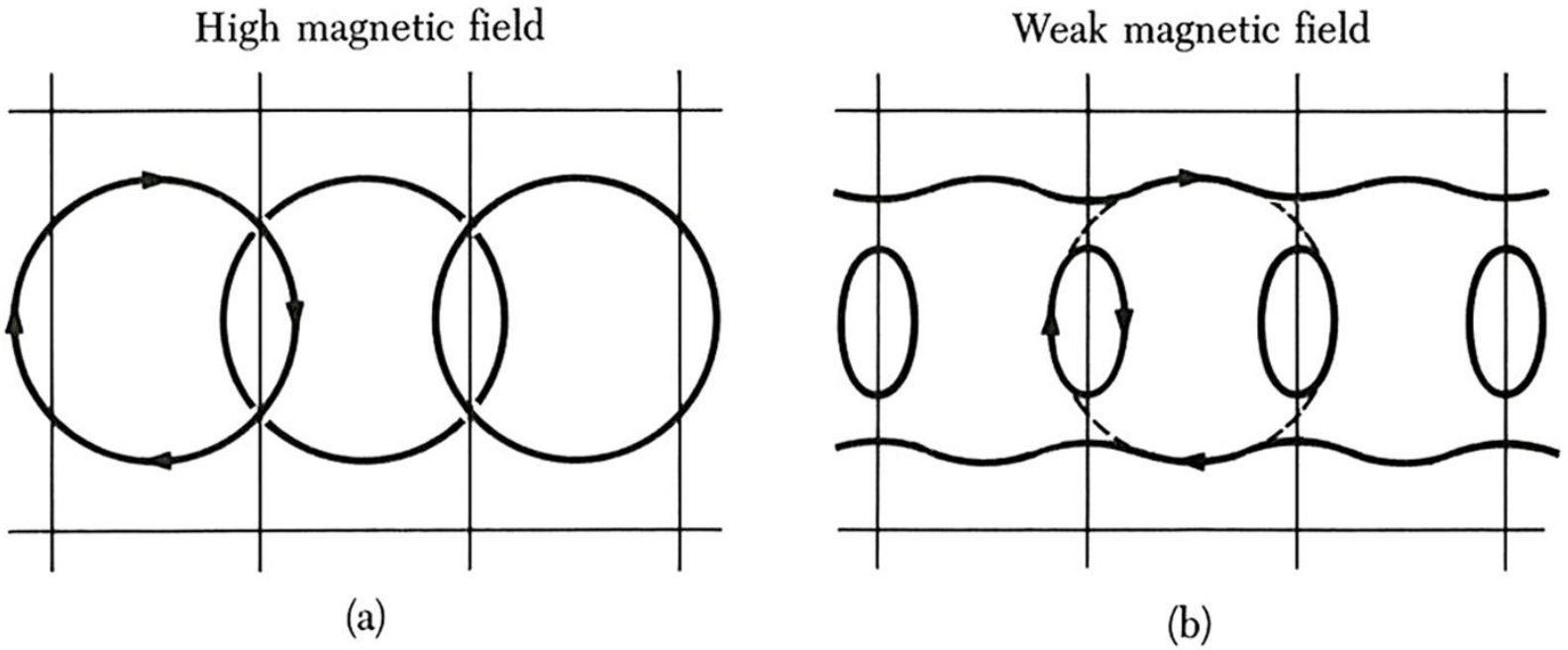

Figure 33 Breakdown of band structure by a strong magnetic field. Brillouin zone boundaries are the light lines. The free electron orbits (a) in a strong field change connectivity in a weak field (b) to become open orbits in the first band and electron orbits in the second band. Both bands are mapped together.

The eventual breakdown of this description as the magnetic field is increased is called magnetic breakdown.[2] The passage to strong magnetic fields may drastically change the connectivity of the orbits, as in the figure. The onset of magnetic breakdown will be revealed by physical properties such as magnetoresistance that depend sensitively on the connectivity.

The condition for magnetic breakdown is that $\hbar\omega_c\epsilon_F > E_g^2$, approximately. Here ϵ_F is the free electron Fermi energy and E_g is the energy gap. This condition is much milder, especially in metals with small gaps, than the naïve condition that the magnetic splitting $\hbar\omega_c$ exceed the gap.

Small gaps may be found in hcp metals where the gap across the hexagonal face of the zone would be zero except for a small splitting introduced by the spin-orbit interaction. In Mg the splitting is of the order of 10^{-3} eV; for this gap and $\epsilon_F \sim 10$ eV the breakdown condition is $\hbar\omega_c > 10^{-5}$ eV, or $B > 1000$ G.